Biochimica et Biophysica Acta 1798 (2010) 312–317

Contents lists available at ScienceDirect

Biochimica et Biophysica Acta

journal homepage: www.elsevier.com/locate/bbamem

^{15}N Solid-state NMR spectroscopic studies on phospholamban at its phosphorylated form at Ser-16 in aligned phospholipid bilayers

Shidong Chu, Shadi Abu-Baker, Junxia Lu, Gary A. Lorigan *

Department of Chemistry and Biochemistry, Miami University, Oxford, Ohio 45056, USA

ARTICLE INFO

Article history:
Received 11 March 2009
Received in revised form 18 December 2009
Accepted 22 December 2009
Available online 4 January 2010

Keywords:
Phospholamban
Protein phosphorylation
Solid-state NMR
Mechanically oriented bilayer

ABSTRACT

Wild-type phospholamban (WT-PLB) is a pentameric transmembrane protein that regulates the cardiac cycle (contraction and relaxation). From a physiological prospective, unphosphorylated WT-PLB inhibits sarcoplasmic reticulum ATPase activity; whereas, its phosphorylated form relieves the inhibition in a mechanism that is not completely understood. In this study, site-specifically ^{15}N-Ala-11- and ^{15}N-Leu-7-labeled WT-PLB and the corresponding phosphorylated forms (P-PLB) were incorporated into 1,2-dioleoyl-*sn*-glycero-3-phosphocholine/2-dioleoyl-*sn*-glycero-3-phosphoethanolamine (DOPC/DOPE) mechanically oriented lipid bilayers. The aligned ^{15}N-labeled Ala-11 and Leu-7 WT-PLB samples show ^{15}N resonance peaks at approximately 71 ppm and 75 ppm, respectively, while the corresponding phosphorylated forms P-PLB show ^{15}N peaks at 92 ppm and 99 ppm, respectively. These ^{15}N chemical shift changes upon phosphorylation are significant and in agreement with previous reports, which indicate that phosphorylation of WT-PLB at Ser-16 alters the structural properties of the cytoplasmic domain with respect to the lipid bilayers.

Published by Elsevier B.V.

1. Introduction

Wild-type phospholamban (WT-PLB, 52 amino acid transmembrane protein) plays a major role in the regulation process of the cardiac cycle (contraction and relaxation), which controls the heartbeat [1]. Using ^{2}H ss-NMR spectroscopy, it has been reported that WT-PLB forms a pentamer in phosphatidylcholine (PC) membranes [2]. From a physiological prospective, unphosphorylated WT-PLB inhibits sarcoplasmic reticulum ATPase activity and this inhibition can be relieved (i.e. reestablishes Ca^{2+} flow) by the cyclic AMP- and calmodulin-dependent phosphorylation of WT-PLB [1]. Since WT-PLB plays a major physiological role, several theoretical and biophysical experimental studies have been conducted to probe its structure and dynamics embedded into a membrane [3–34].

Early structural studies on WT-PLB disagreed on whether the pentameric form of the protein is composed of five continuous α-helical subunits or subunits that have two α-helices connected by an unstructured/β-sheet region [3,4]. A solution NMR structural study by the Chou group indicated that pentameric WT-PLB forms a bellflower-like structural assembly in micelles, in which the α-helical cytoplasmic domain of the pentamer on average points away from the membrane surface [8]. Conversely, the Thomas group has indicated that the cytoplasmic domain of each subunit of the WT-PLB is in direct contact with the membrane surface forming an L-shaped pinwheel geometry using fluorescence resonance energy transfer (FRET) [5]. Clearly, the structural topology of pentameric WT-PLB and its interaction with the membrane have been under serious debate. Two recent structural studies on WT-PLB from the Lorigan [35] and the Veglia and Thomas [36] labs have been conducted independently and both reports conclude that the cytoplasmic domain of each subunit of WT-PLB is in direct contact with the membrane surface forming an L-shaped pinwheel geometry in POPC/POPE membranes. In agreement with this model, two earlier NMR studies suggested that a direct interaction takes place between the cytoplasmic domain of the full-length WT-PLB and the phospholipid head groups of the bilayers [6,7].

Similarly, another debate has been reported on the physiologically active monomeric AFA-PLB mutant (AFA-PLB), in which all three native transmembrane (TM) cysteines have been replaced by A36, F41, and A46. The Veglia [9,10] and Baldus [37] groups, respectively, disagree whether the monomeric AFA-PLB mutant structure has an α-helical cytosolic segment that lies on and interacts with the membrane surface (L-shaped structure) or a non-α-helical disordered cytosolic domain that has minimal interaction with the DOPC/DOPE membrane surface. Also, the effect of phosphorylation on the structural topology of the cytoplasmic domain of the monomeric AFA-PLB mutant has

Abbreviations: CSA, chemical shift anisotropy; CP-MAS, Cross-polarization magic angle spinning; DOPC, 1,2-dioleoyl-*sn*-glycero-3-phosphocholine; DOPE, 1,2-dioleoyl-*sn*-glycero-3-phosphoethanolamine; POPC, 1-palmitoyl-2-oleoyl-*sn*-glycerophosphocholine; POPE, 1-palmitoyl-2-oleoyl-*sn*-glycero-3-phosphoethanolamine; P-PLB, phosphorylated phospholamban; WT-PLB, wild-type phospholamban; SERCA, sarco (endo) plasmic reticulum calcium ATPase; MLVs, multilamellar vesicles

* Corresponding author. Tel.: +1 513 529 3338; fax: +1 513 529 5715.
E-mail address: garylorigan@muohio.edu (G.A. Lorigan).

0005-2736/$ – see front matter. Published by Elsevier B.V.
doi:10.1016/j.bbamem.2009.12.020

been probed by the Veglia and Bigelow groups [38,39]. The Veglia group indicated that phosphorylation of Ser-16 (located within the cytoplasmic domain) induces an order-to-disorder transition that disrupts the "L-shaped" AFA-PLB monomer and causes a reduction in the α-helical secondary structure around the phosphorylation site [38]. This finding contradicts the research by Bigelow et al. which suggested that phosphorylation of AFA-PLB increases the stabilization of the helical content, especially in the hinge region, leaving the cytoplasmic domain associated with the membrane [39].

In the case of pentameric WT-PLB, the effect of phosphorylation on the structural topology of the cytoplasmic domain is not well understood. Articles describing changes in the dynamics and structural topology of the cytoplasmic domain upon phosphorylation in the presence and/or absence of SERCA have resulted in different models describing the interaction of PLB with SERCA [1,8,40].

In a recent study, we showed using ^{13}C cross-polarization magic angle spinning (CP-MAS) solid-state NMR (ss-NMR) experiments that Ala-15 (closest to the phosphorylation site) representing the cytoplasmic domain is part of an α-helical structure with and without Ser-16 phosphorylation [6]. In another study, ^{2}H and ^{15}N ss-NMR spectroscopic techniques were used to investigate both the side chain and backbone dynamics of wild-type phospholamban (WT-PLB) and its phosphorylated form (P-PLB) incorporated into 1-palmitoyl-2-oleoyl-*sn*-glycerophosphocholine (POPC) phospholipid multilamellar vesicles (MLVs) [41]. Additionally, we used ^{15}N ss-NMR spectroscopy to ascertain direct information regarding the structural topology of the site-specific ^{15}N-labeled WT-PLB pentamer in oriented phospholipid bilayers, and the alignment of each helix with respect to the bilayer normal has been determined [35]. In this report, we extend and complement our previous dynamic and structural studies using ^{15}N and ^{31}P ss-NMR spectroscopy on site-specifically ^{15}N-labeled WT-PLB and P-PLB (phosphorylated at Ser-16) embedded into oriented phospholipid bilayers.

2. Materials and methods

2.1. Materials

All synthetic phospholipids were purchased from Avanti Polar Lipids (Alabaster, AL). The phospholipids were dissolved in chloroform and stored at −20 °C before use. Trifluoroethanol (TFE), N-[2-hydroxyethyl] piperazine-N′-2-ethane sulfonic acid (HEPES) and acrylamide were obtained from Sigma-Aldrich (St. Louis, MO). Fmoc amino acids, prephosphorylated Ser Fmoc derivative, and other chemicals for peptide synthesis were purchased from Novabiochem (San Diego, CA). ^{15}N-L-Ala N-Fmoc derivative, ^{15}N-L-Leu N-Fmoc derivative, $^{15}NH_4Cl$, and deuterium-depleted water were purchased from Isotec™/Sigma-Aldrich (Miamisburg, OH). Precise™ protein pre-cast gels and protein standards for sodium dodecyl sulfate polyacrylamide gel electrophoresis (SDS-PAGE) were purchased from Thermo Scientific (Rockford, IL) and Invitrogen (Carlsbad, CA), respectively.

2.2. Synthesis, purification and characterization of ^{15}N-labeled WT-PLB and P-PLB

The peptides were ^{15}N-labeled at the Ala-11 or Leu-7 positions, synthesized using a modified Fmoc-based solid-phase synthesis method and purified with preparative HPLC using a reverse phase polymer column as reported previously [6]. The uniformly ^{15}N-labeled WT-PLB was over-expressed and purified as described previously [42] with a slightly modified procedure as reported earlier [41]. The proteins were lyophilized and characterized by matrix-assisted laser desorption ionization time-of-flight (MALDI-TOF) mass spectrometry and SDS-PAGE. SDS-PAGE of WT-PLB and P-PLB were conducted according to Wegener and Jones [47] using a 4 to 15% acrylamide gradient in the resolving gel. After electrophoresis, the gel was stained for 30 min with Coomassie Blue followed by overnight destaining.

2.3. NMR sample preparation

For ^{15}N NMR experiments, mechanically aligned samples containing site-specifically ^{15}N-labeled WT-PLB or P-PLB in a mixture of 1,2-dioleoyl-*sn*-glycero-3-phosphocholine (DOPC) and 1,2-dioleoyl-*sn*-glycero-3-phosphoethanolamine (DOPE) lipids (4:1 ratio) were prepared as described previously [44]. Briefly, about 4–5 mg of ^{15}N-labeled peptide was first dissolved in a minimal amount of TFE prior to cosolubilizing with 60 mg of the DOPC/DOPE lipids (peptide: lipid at a 1:100 mol ratio). The volume of the solution was reduced under a stream of nitrogen gas to about 1 mL before any lipid or peptide precipitated. The solution was separated onto 35 (5.7×12 mm) glass plates and allowed to air-dry for 30 min before vacuum drying overnight. Deuterium-depleted water was added onto the peptide/lipid mixture (4 μL/plate), and the glass plates were stacked carefully on top of each other. The stacked glass plates were then placed in a humidity chamber consisting of saturated ammonium mono phosphate at a relative humidity of about 93% at 42 °C for 12 h. The glass plates were then placed into a rectangular thin-wall glass cell with one-pre-sealed end and the sample cell was sealed with wax before placing it into the sample NMR coil.

The DOPC/DOPE lipid combination has been used for functional reconstitution of WT-PLB into lipid membranes as determined by Ca^{2+}-ATPase activity [45]. The aligned samples were first used in the ^{31}P ss-NMR experiments to evaluate the alignment of the lipid bilayers.

2.4. Solid-state NMR spectroscopy

A Bruker AVANCE 500 MHz (11.7 T) wide-bore NMR spectrometer (Bruker, Billerica, MA) and a flat coil ^{1}H-X Low-E NMR probe (NMR Instruments Development Group, NHMFL, Tallahassee, FL) with coil dimensions 7.6×5.6×11 mm were used to collect the static ^{15}N CP and ^{31}P NMR spectra [46].

The ^{31}P NMR spectra were recorded with ^{1}H decoupling using a 4.0 μs 90° pulse for ^{31}P and a 4.0 s recycle delay. The spectral width was set to 250 ppm. For the ^{31}P NMR spectra 128 scans were taken and the free induction delay was processed using 100 Hz of line broadening. All ^{31}P NMR spectra were referenced by assigning the 85% H_3PO_4 ^{31}P peak to 0 ppm.

Static ^{15}N ss-NMR spectra were collected utilizing a RAMP cross-polarization pulse sequence with ^{1}H decoupling. The following pulse sequence parameters were used: 5.0 μs ^{1}H 90° pulse, 1.5 ms contact time, 500 ppm sweep width, a 4.0 s recycle delay, and a proton B_1 field strength of ~50 kHz. Also, 120 K scans were averaged for the static ^{15}N CP experiments and the free induction delay was processed using 300 Hz of line broadening. The ^{15}N CP NMR spectra were referenced to an external standard of $(^{15}NH_4)_2SO_4$ (27 ppm).

For all the aligned samples, the radiofrequency (RF) coil was adjusted so that the lipid bilayer normal was aligned parallel with the static magnetic field B_0. All the ss-NMR experiments were conducted at 25 °C.

3. Results

3.1. Electrophoresis analysis of PLB phosphorylation

The oligomeric states of both WT-PLB and P-PLB were examined using SDS-polyacrylamide gel electrophoresis in Fig. 1. Both WT-PLB and P-PLB are predominantly in the pentameric state on SDS-PAGE gels, and do not show the coexistence of any significant amounts of monomeric or dimeric forms as reported for the monomeric forms (AFA-PLB) [25,43]. The gel matches very well with previous studies carried out by the Jones [47] and Thomas groups [48], in which P-PLB migrates slower than WT-PLB due to decreased mobility. The shifted P-PLB band shows up at a higher apparent molecular weight, upon comparison with the WT-PLB band.

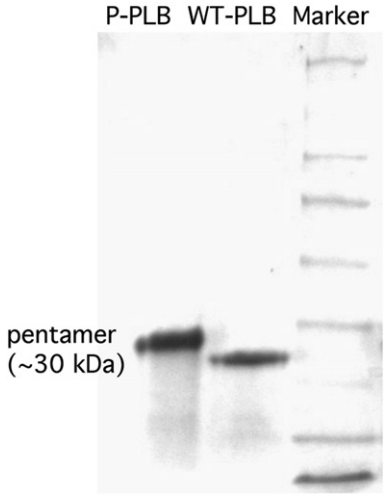

Fig. 1. SDS-PAGE gels of WT-PLB and P-PLB. From left to right: P-PLB, WT-PLB, and the molecular weight marker.

As reported early, PLB behaves similarly in response to phosphorylation in both detergent and lipid bilayers [48]. The Smith group [2] has demonstrated with ss-NMR spectroscopy that the full-length WT-PLB forms a pentamer in PC membranes and a similar conclusion was reported in our previous transmembrane PLB (TM-PLB) studies [44]. Recent NMR studies have also suggested that a phosphorylation-mimicking mutation does not perturb the pentameric structure of PLB in DPC micelles [49].

3.2. The alignment of PLB in DOPC/DOPE bilayers

Fig. 2 shows the ^{31}P NMR spectra of mechanically aligned DOPC/DOPE (4:1 ratio) bilayers in the absence and presence of 1 mol% WT-PLB and P-PLB. The results indicate that uniformly aligned DOPC/DOPE lipid bilayers with ^{31}P resonance peaks at ~26 ppm were formed in the presence and absence of 1 mol% peptide. The well-resolved ^{31}P peak at ~26 ppm indicates that the phospholipid bilayers are well aligned such that the bilayer normal is parallel with the static magnetic field. The linewidths at half height of the ^{31}P NMR resonances are less than 1 ppm for the pure lipids and about 2.5 ppm for lipids containing 1 mol % peptide.

^{31}P NMR is effective for evaluating the quality of macroscopic membrane alignment. ^{15}N NMR resonance peaks from amide proteins are also a direct indicator of the protein alignment in the membranes and necessary for assessing the quality of sample alignment. One-dimensional ^{15}N ss-NMR spectra of uniformly ^{15}N-labeled proteins can also be used to monitor and optimize alignment conditions. As shown in Fig. 3A, the dip in the baseline at ~147 ppm of the ^{15}N NMR spectrum of uniformly ^{15}N-labeled WT-PLB in aligned DOPC/DOPE (4:1) glass plates is indicative of a well-oriented membrane protein sample, because no ^{15}N powder pattern components of significant amount are observed [50].

3.3. ^{15}N solid-state NMR of WT-PLB and P-PLB in aligned DOPC/DOPE bilayers

The topological orientation and dynamics of PLB, especially the cytoplasmic domain, is believed to play a crucial role in the regulation of the Ca^{2+} pump SERCA, in which the working mechanism is still not fully understood [1,3–10,37–40]. SS-NMR spectroscopy of macroscopically aligned proteins provides an important method to determine the orientation of proteins in membranes and has been extensively used in NMR studies of membrane proteins [35,36,50,51,53,55–62]. In order to probe the effect of phosphorylation on the structural topology of the cytoplasmic domain of WT-PLB, site-specifically ^{15}N-labeled amide

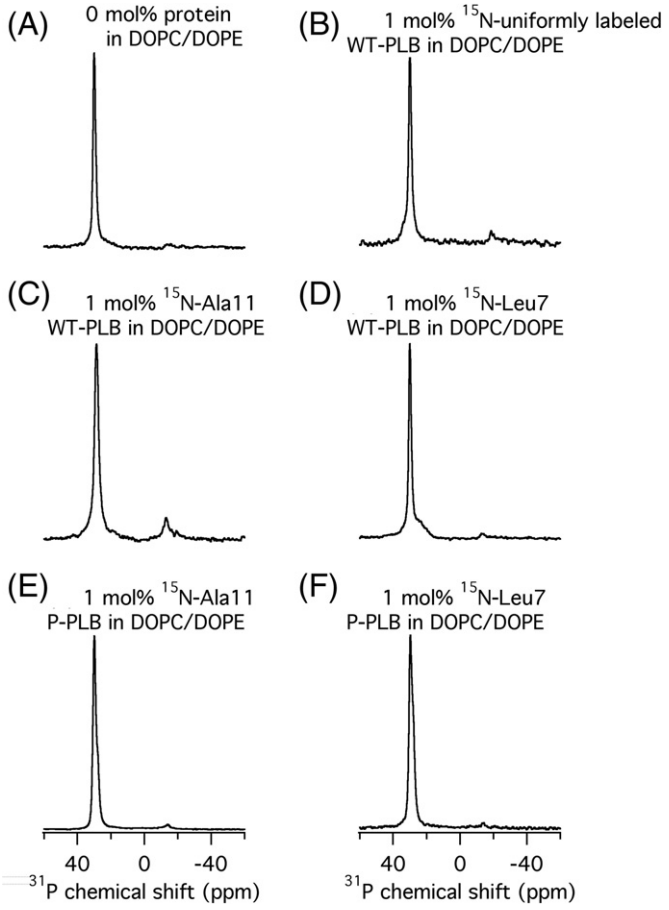

Fig. 2. ^{31}P solid-state NMR spectra of aligned DOPC/DOPE (4:1 ratio) bilayers in the presence of 0 mol% (A), 1 mol% of ^{15}N-uniformly-labeled PLB (B), ^{15}N-Ala-11 labeled WT-PLB (C) and P-PLB (E), ^{15}N-Leu-7 labeled WT-PLB (D) and P-PLB (F), respectively.

residues located on the cytoplasmic domain (Ala-11 and Leu-7) of WT-PLB and P-PLB were prepared and incorporated into aligned DOPC/DOPE bilayers respectively and analyzed via ^{15}N ss-NMR spectroscopy.

Fig. 3 shows the one-dimensional static ^{15}N ss-NMR spectra of uniformly ^{15}N-labeled WT-PLB as well as site-specifically ^{15}N-labeled WT-PLB (Ala-11 and Leu-7) and their corresponding phosphorylated forms (P-PLB) embedded inside mechanically aligned DOPC/DOPE (4:1) phospholipids using glass plates. As in agreement with other studies, the uniformly ^{15}N-labeled WT-PLB spectrum shows two distinct components at ~73 ppm and at ~211 ppm (Fig. 3A). In a recent study, we showed using site-specifically ^{15}N-labeled amide residues located on both the cytoplasmic domain (Ala-11) and the transmembrane domain (Leu-42 and Leu-51) of WT-PLB that the component at 211 ppm (near $\sigma_{||}$) belongs to the transmembrane domain (nearly parallel with B_0), whereas the component at 73 ppm (near $\sigma_{\perp}$) corresponds to the cytoplasmic domain of WT-PLB which lies on the membrane surface [35].

The ^{15}N-labeled Ala-11 WT-PLB and P-PLB samples show ^{15}N resonance peaks at approximately 71 ppm and 92 ppm, respectively (Fig. 3B and C). Similarly, ^{15}N-labeled Leu-7 samples of WT-PLB and P-PLB reveal ^{15}N resonance peaks at about 75 ppm and 99 ppm, respectively (Fig. 3D and E). The ^{15}N resonances linewidths of the aligned site-specifically ^{15}N-labeled peptides are about 15 ppm, with the broadest peak of 17.8 ppm for ^{15}N-Leu-7 P-PLB. The ^{15}N linewidths for the aligned peptides in Fig. 3B–E are in the range of 15 to 20 ppm, which were observed in many aligned peptides in lipid membranes [51,62]. The ^{15}N-labeled Ala-11 and Leu-7 resonance peaks of WT-PLB are very close to the $\sigma_{\perp}$ component (73 ppm) of the ^{15}N CSA tensor of the corresponding powder spectrum, indicating that these two residues

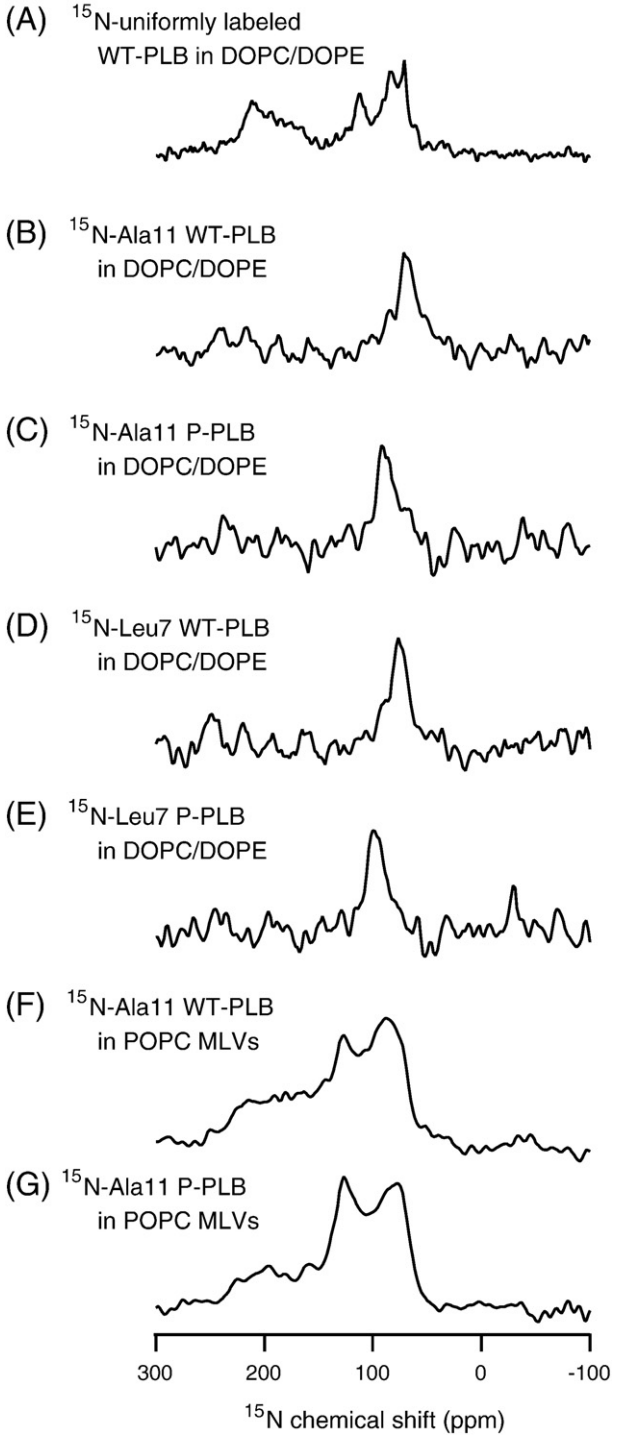

Fig. 3. ^{15}N cross-polarization NMR spectra of uniformly ^{15}N-labeled WT-PLB (A) as well as site-specifically ^{15}N-labeled WT-PLB at Ala-11 (B) or Leu-7 (D), and P-PLB at Ala-11 (C) or Leu-7 (E) in oriented DOPC/DOPE (4:1 ratio) lipid bilayers. The ^{15}N NMR powder spectra of WT-PLB (F) and P-PLB (G) in POPC MLVs are also presented.

located in the cytoplasmic domain are oriented approximately perpendicular to the bilayer normal (sitting on the bilayer surface). This data agrees with previous NMR studies by the Veglia, Thomas, and Lorigan research groups on AFA-PLB and WT-PLB [35,36].

4. Discussion

Interestingly, the aligned ^{15}N resonance peaks of ^{15}N-labeled Ala-11 and Leu-7 of P-PLB are shifted downfield by more than 20 ppm when compared to the residue peaks of the corresponding WT-PLB samples (Fig. 3B–E). These 20 ppm shifts are significant and may be due to several different factors (a) the negative charge on the Ser-16 residue after phosphorylation, (b) significant backbone dynamic changes in WT-PLB upon phosphorylation, and (c) structural perturbations induced by phosphorylation.

If the 20 ppm shifts were induced by the introduction of the negative charge on Ser-16 upon phosphorylation, the ^{15}N isotropic CP-MAS and the corresponding ^{15}N CSA values would also be altered. The ^{15}N CP-MAS NMR spectra of ^{15}N-labeled Ala-11 WT-PLB and P-PLB both yield the same isotropic CSA value of approximately 121 ppm (data not shown) [41]. Furthermore, as seen in Fig. 3F–G, the ^{15}N static powder pattern NMR spectra of both samples are fairly comparable with the following CSA values: σ_{11} (58 ppm and 60 ppm), σ_{22} (76 ppm and 73 ppm) and σ_{33} (230 ppm and 229 ppm) for WT-PLB and P-PLB, respectively [41]. Thus, this shift is not caused by the phosphorylation charge on Ser-16.

If the ~20 ppm shifts observed in the aligned samples for the dominant form of P-PLB were solely due to dynamic motion of the cytoplasmic domain upon phosphorylation, the ^{15}N CSA values of the powder pattern spectrum would also decrease by approximately 20 ppm ($\sigma_{33}-\sigma_{11}$) as well. This phenomenon can be observed in the literature, ^{15}N NMR spectra of both oriented and unoriented peptides show a reduced ^{15}N CSA when compared with that of rigid proteins, indicating that the peptide undergoes uniaxial rotation around the bilayer normal with correlation times faster than 10^{-4} s [52]. However, as indicated previously, the ^{15}N powder pattern CSA width ($\sigma_{33}-\sigma_{11}$) values of P-PLB do not change by ~20 ppm. The ^{15}N CSA powder pattern spectra of ^{15}N-labeled P-PLB and WT-PLB have two components (Fig. 3F–G), which indicate a slight increase in backbone motion for P-PLB over WT-PLB [41]. The width of the broad axial symmetric dominant component is slightly smaller ($\sigma_{33}-\sigma_{11}=3$ ppm), when compared to WT-PLB. The isotropic component of P-PLB is slightly larger when compared to WT-PLB [41]. It should be noted that the aligned NMR spectra presented in this paper were prepared on glass plates, whereas the unoriented "powder pattern" spectra were collected in MLVs. If the ~20 ppm ^{15}N shift were due to backbone dynamics from the cytoplasmic domain alone, one would expect to observe even more dynamic averaging of the CSA values in the MLV samples, because the bilayers are more hydrated than the corresponding aligned glass plate samples. These large ^{15}N shift dynamic differences are not observed in the P-PLB samples. In summary, we do observe slight ^{15}N backbone dynamic differences (~3 ppm ^{15}N shift) between P-PLB and WT-PLB but not enough to account for ~20 ppm ^{15}N shift.

The 20 ppm ^{15}N shift observed in the P-PLB samples is most likely due to structural perturbations induced by phosphorylation. The structural changes may consist of one or a combination of the following: (a) secondary structural changes in the cytoplasmic domain of P-PLB, (b) changes in the oligomeric structure of P-PLB, or (c) changes in the tilt and/or rotation angles of the cytoplasmic helix upon phosphorylation.

Significant changes in the secondary structural conformation upon phosphorylation are not supported by previous ss-NMR data on the cytoplasmic domain of P-PLB and WT-PLB at positions Ala-11 and Ala-15 [6,41]. ^{15}N CP-MAS isotropic values of ^{15}N-labeled amide residues at Ala-11 are consistent with an α-helical structure for both WT-PLB and P-PLB [41]. In another study, ^{13}C CP-MAS ss-NMR spectra indicate that Ala-15 (closest to the phosphorylation site Ser-16) representing the cytoplasmic domain is still a part of an α-helical structure after phosphorylation at Ser-16 [6].

The introduction of a negatively-charged phosphate group at Ser-16 could alter the oligomerization state of PLB, promoting PLB pentamer formation slightly in lipid bilayers [48]. As shown in Fig. 1, both WT-PLB and P-PLB are predominantly in the pentameric state. We only observe a single ^{15}N peak for both Ala-11 and Leu-7 in the WT-PLB and P-PLB samples. The ^{15}N peaks observed most likely are from the dominant pentameric form of the protein.

Generally, helical tilt and rotational motions of most helices in a membrane are constrained by their tertiary structure, oligomerization state and/or interaction with the lipid bilayers [53]. The ^{15}N NMR spectrum of the aligned ^{15}N uniformly-labeled PLB in Fig. 3A indicates that protein backbone dynamics are on the 10^4 Hz time scale of the ^{15}N amide chemical shift interaction [50]. Rotation about the peptide long axis is almost static on the NMR time scale of 10^{-4} s [54]. Based upon ^{15}N ss-NMR studies of peptides aligned almost parallel with the membrane surface, rotation alone is unlikely to cause the ^{15}N resonance peaks to shift from ~70 ppm to 90–100 ppm [55–59]. Previous studies by the Veglia group have shown that the cytoplasmic segment of the dominant pentameric form of WT-PLB lays on the surface of DOPC/DOPE membranes [36]. In that paper, the ^{15}N resonance peaks for the aligned cytoplasmic domain of WT-PLB range from approximately 65 to 82 ppm [36]. The ^{15}N peaks presented in this paper for Ala-11 (71 ppm) and Leu-7 (75 ppm) clearly fall into the range observed for WT-PLB by the Veglia group. If upon phosphorylation, the cytoplasmic domain rotated about the surface of the bilayer one would expect the ^{15}N values to potentially change, but still vary between 65 and 82 ppm. Clearly, the ~20 ppm shift that we observe for the P-PLB samples falls outside the range observed by the Veglia group for the cytoplasmic domain of WT-PLB.

One reasonable explanation for the ~20 ppm ^{15}N chemical shift upon phosphorylation may be a helical tilt change in which the helical orientation of P-PLB shifts away from the bilayer surface when compared with WT-PLB. Based upon the 20 ppm ^{15}N shift, the helix would move about 15° from the surface of the bilayer [55]. Notably, the membrane association of helix 2 of the HIV-1 viral protein U (Vpu) was also shown to be weakened by phosphorylation using aligned ss-NMR spectroscopic techniques [60]. As anticipated with this tilt, the ^{15}N chemical shift of ^{15}N-Leu-7 is slightly larger than that of ^{15}N-Ala-11, because Leu-7 is closer to the end of the cytoplasmic helix than Ala-11. The interpretation of this data fits well with the allosteric activation model of PLB by the Veglia and Thomas groups [40]. Furthermore, we have shown using ^{31}P NMR spectroscopy that WT-PLB and P-PLB interact differently in MLVs [6]. In that study, P-PLB interacted less with the phospholipid headgroups, when compared to WT-PLB. If the helix of the cytoplasmic domain shifted away from the membrane surface, one would expect less interaction with the phospholipid headgroups. Thus, the lipid-protein interactions probed with ^{31}P NMR agree with the protein^{15}N NMR results presented in this study. The ^{15}N NMR differences observed in this paper between WT-PLB and P-PLB are most likely due to either structural perturbations or a combination of structural and slight dynamic backbone changes upon phosphorylation.

Acknowledgements

We acknowledge the helpful support on the preparation of ^{15}N uniformly-labeled WT-PLB from the research labs of Dr. Gianluigi Veglia and Dr. David Thomas at the University of Minnesota. We would like to thank Dr. Thusitha Gunasekera for the help with the SDS-PAGE gels. This work was supported by a NIH grant (GM080542) and an AHA grant (0755602B). The Bruker 500 MHz wide-bore NMR spectrometer was obtained from a NSF grant (10116333).

References

[1] H.K.B. Simmerman, L.R. Jones, Phospholamban: protein structure, mechanism of action, and role in cardiac function, Physiol. Rev. 78 (1998) 921–947.
[2] W. Ying, S.E. Irvine, R.A. Beekman, D.J. Siminovitch, S.O. Smith, Deuterium NMR reveals helix packing interactions in phospholamban, J. Am. Chem. Soc. 122 (2000) 11125–11128.
[3] I.T. Arkin, M. Rothman, C.F.C. Ludlam, S. Aimoto, D.M. Engelman, K.J. Rothschild, S.O. Smith, Structural model of the phospholamban ion-channel complex in phospholipid-membranes, J. Mol. Biol. 248 (1995) 824–834.
[4] S.A. Tatulian, L.R. Jones, L.G. Reddy, D.L. Stokes, L.K. Tamm, Secondary structure and orientation of phospholamban reconstituted in supported bilayers from polarized attenuated total-reflection FTIR spectroscopy, Biochemistry 34 (1995) 4448–4456.
[5] S.L. Robia, N.C. Flohr, D.D. Thomas, Phospholamban pentamer quaternary conformation determined by in-gel fluorescence anisotropy, Biochemistry 44 (2005) 4302–4311.
[6] S. Abu-Baker, G.A. Lorigan, Phospholamban and its phosphorylated form interact differently with lipid bilayers: A ^{31}P, ^{2}H, and ^{13}C solid-state NMR spectroscopic study, Biochemistry 45 (2006) 13312–13322.
[7] J.C. Clayton, E. Hughes, D.A. Middleton, The cytoplasmic domains of phospholamban and phospholemman associate with phospholipid membrane surfaces, Biochemistry 44 (2005) 17016–17026.
[8] K. Oxenoid, J.J. Chou, The structure of phospholamban pentamer reveals a channel-like architecture in membrane, Proc. Natl. Acad. Sci. USA 102 (2005) 10870–10875.
[9] A. Mascioni, C. Karim, J. Zamoon, D.D. Thomas, G. Veglia, Solid-state NMR and rigid body molecular dynamics to determine domain orientations of monomeric phospholamban, J. Am. Chem. Soc. 124 (2002) 9392–9393.
[10] J. Zamoon, A. Mascioni, D.D. Thomas, G. Veglia, NMR solution structure and topological orientation of monomeric phospholamban in dodecylphosphocholine micelles, Biophys. J. 85 (2003) 2589–2598.
[11] N.J. Traaseth, K.N. Ha, R. Verardi, L. Shi, J.J. Buffy, L.R. Masterson, G. Veglia, Structural and dynamic basis of phospholamban and sarcolipin inhibition of Ca^{2+}-ATPaset, Biochemistry 47 (2008) 3–13.
[12] T. Morita, D. Hussain, M. Asahi, T. Tsuda, K. Kurzydlowski, C. Toyoshima, D.H. MacLennan, Interaction sites among phospholamban, sarcolipin, and the sarco (endo)plasmic reticulum Ca^{2+}-ATPase, Biochem. Biophys. Res. Commun. 369 (2008) 188–194.
[13] W. Liu, J.Z. Fei, T. Kawakami, S.O. Smith, Structural constraints on the transmembrane and juxtamembrane regions of the phospholamban pentamer in membrane bilayers: Gln29 and Leu52, Biochim. Biophys. Acta -Biomembranes 1768 (2007) 2971–2978.
[14] K.N. Ha, N.J. Traaseth, R. Verardi, J. Zamoon, A. Cembran, C.B. Karim, D.D. Thomas, G. Veglia, Controlling the inhibition of the sarcoplasmic Ca^{2+}-ATPase by tuning phospholamban structural dynamics, J. Biol. Chem. 282 (2007) 37205–37214.
[15] Y.E. Nesmelov, C.B. Karim, L. Song, P.G. Fajer, D.D. Thomas, Rotational dynamics of phospholamban determined by multifrequency electron paramagnetic resonance, Biophys. J. 93 (2007) 2805–2812.
[16] L.M. Espinoza-Fonseca, D. Kast, D.D. Thomas, Molecular dynamics simulations reveal a disorder-to-order transition on phosphorylation of smooth muscle myosin, Biophys. J. 93 (2007) 2083–2090.
[17] N.J. Traaseth, J.J. Buffy, J. Zamoon, G. Veglia, Structural dynamics and topology of phospholamban in oriented lipid bilayers using multidimensional solid-state NMR, Biochemistry 45 (2006) 13827–13834.
[18] E.S. Karp, E.K. Tiburu, S. Abu-Baker, G.A. Lorigan, The structural properties of the transmembrane segment of the integral membrane protein phospholamban utilizing C-13 CP-MAS, H-2, and REDOR solid-state NMR spectroscopy, Biochim. Biophys. Acta -Biomembranes 1758 (2006) 772–780.
[19] C.B. Karim, Z.W. Zhang, E.C. Howard, K.D. Torgersen, D.D. Thomas, Phosphorylation-dependent conformational switch in spin-labeled phospholamban bound to SERCA, J. Mol. Biol. 358 (2006) 1032–1040.
[20] P.D. Adams, I.T. Arkin, D.M. Engelman, A.T. Brunger, Computational searching and mutagenesis suggest a structure for the pentameric transmembrane domain of phospholamban, Nat. Struct. Biol. 2 (1995) 154–162.
[21] I.T. Arkin, P.D. Adams, A.T. Brunger, S.O. Smith, D.M. Engelman, Structural perspectives of phospholamban, a helical transmembrane pentamer, Annu. Rev. Biophys. Biomol. Struct. 26 (1997) 157–179.
[22] J. Fuji, A. Ueno, K. Kitano, S. Tanaka, M. Kadoma, M. Tada, Characterization of structural unit of phospholamban by amino acid sequencing and electropherotic analysis, Biochem. Biophys. Res. Commun. 138 (1987) 1044–1050.
[23] Y. Houndonougbo, K. Kuczera, G.S. Jas, Structure and dynamics of phospholamban in solution and in membrane bilayer: Computer simulations, Biochemistry 44 (2005) 1780–1792.
[24] J.A. Hubbard, L.K. Maclachlan, E. Meenan, C.J. Salter, D.G. Reid, P. Lahouratate, J. Humphries, N. Stevens, D. Bell, W.A. Neville, K.J. Murray, J.G. Darker, Conformation of the cytoplasmic domain of phospholamban by NMR and CD, Mol. Mem. Biol. 11 (1994) 263–269.
[25] E. Hughes, J.C. Clayton, D.A. Middleton, Probing the oligomeric state of phospholamban variants in phospholipid bilayers from solid-state NMR measurements of rotational diffusion rates, Biochemistry 44 (2005) 4055–4066.
[26] E. Hughes, D.A. Middleton, Solid-state NMR reveals structural changes in phospholamban accompanying the functional regulation of Ca^{2+}-ATPase, J. Biol. Chem. 278 (2003) 20835–20842.
[27] R.J. Kovacs, M.T. Nelson, H.B.K. Simmerman, L.R. Jones, Phospholamban forms calcium selective channels in lipid bilayers, J. Biol. Chem. 263 (1988) 18364–18368.
[28] S. Lamberth, H. Schmid, M. Muenchbach, T. Vorherr, J. Krebs, E. Carafoli, C. Griesinger, NMR solution structure of phospholamban, Helvet. Chim. Acta 83 (2000) 2141–2152.
[29] H.M. Li, M.J. Cocco, T.A. Steitz, D.M. Engelman, Conversion of phospholamban into a soluble pentameric helical bundle, Biochemistry 40 (2001) 6636–6645.
[30] J.H. Li, Y.J. Xiong, D.J. Bigelow, T.C. Squier, Phospholamban binds in a compact and ordered conformation to the Ca-ATPase, Biochemistry 43 (2004) 455–463.
[31] N.A. Lockwood, R.S. Tu, Z.W. Zhang, M.V. Tirrell, D.D. Thomas, C.B. Karim, Structure and function of integral membrane protein domains resolved by peptide-amphiphiles: Application to phospholamban, Biopolymers 69 (2003) 283–292.
[32] E.E. Metcalfe, J. Zamoon, D.D. Thomas, G. Veglia, H-1/N-15 heteronuclear NMR spectroscopy shows four dynamic domains for phospholamban reconstituted in dodecylphosphocholine micelles, Biophys. J. 87 (2004) 1205–1214.
[33] B. Mueller, G.W. Hunter, C.B. Karim, D.D. Thomas, FRET detection of Ca-ATPase and phospholamban interaction in membranes, Biophys. J. 84 (2003) 264A.

[34] X.M. Zhang, Y. Kimura, M. Inui, Effects of phospholipids on the oligomeric structure of phospholamban (PLN), a regulator of Ca^{2+}-ATPase of cardiac sarcoplasmic reticulum (SR), J. Pharm. Sci. 94 (2004) 109P.
[35] S. Abu-baker, J. Lu, S. Chu, K.K. Shetty, P.L. Gor'kov, G.A. Lorigan, The structural topology of wild-type phospholamban in oriented lipid bilayers using ^{15}N solid-state NMR spectroscopy, Protein Sci. 16 (2007) 2345–2349.
[36] N.J. Traaseth, R. Verardi, K.D. Torgersen, C.B. Karim, D.D. Thomas, G. Veglia, Spectroscopic validation of the pentameric structure of phospholamban, Proc. Natl. Acad. Sci. U. S. A. 104 (2007) 14676–14681.
[37] C.A. Andronesi, S. Becker, K. Seidel, H. Heise, H.S. Young, M. Baldus, Determination of membrane protein structure and dynamics by magic-angle-spininng solid-state NMR spectroscopy, J. Am. Chem. Soc. 127 (2005) 12965–12974.
[38] E.E. Metcalfe, N.J. Traaseth, G. Veglia, Serine 16 phosphorylation induces an order-to-disorder transition in the monomeric phospholamban, Biochemistry 44 (2005) 4386–4396.
[39] J. Li, D.J. Bigelow, Phosphorylation by cAMP-dependent protien kinase modulates the structural coupling between the transmembrane and cytoplasmic domains of phospholamban, Biochemistry 42 (2003) 10674–10682.
[40] J. Zamoon, F. Nitu, C. Karim, D.D. Thomas, G. Veglia, Mapping the interaction surface of a membrane protein: Unveiling the conformational switch of phospholamban in calcium pump regulation, Proc. Natl. Acad. Sci. U. S. A. 102 (2005) 4747–4752.
[41] S. Abu-baker, J. Lu, S. Chu, C.C. Brinn, C.A. Makaroff, G.A. Lorigan, Side-chain and backbone dynamics of phospholamban in phospholipid bilayers utilizing ^{2}H and ^{15}N solid-state NMR spectroscopy, Biochemistry 46 (2007) 11695–11706.
[42] B. Buck, J. Zamoon, T.L. Kirby, T.M. DeSilva, C. Karim, D. Thomas, G. Veglia, Overexpression, purification, and characterization of recombinant Ca-ATPase regulators for high-resolution solution and solid-state NMR studies, Protein Express. Purif. 30 (2003) 253–261.
[43] H.K.B. Simmerman, D.E. Lovelace, L.R. Jones, Secondary structure of detergent-solubilized phospholamban, a phosphorylatable, oligomeric protein of cardiac sarcoplasmic reticulum, Biochim. Biophys. Acta 997 (1989) 322–329.
[44] E.K. Tiburu, P.C. Dave, K. Damodaran, G.A. Lorigan, Investigating leucine side-chain dynamics and backbone conformations of phospholamban incorporated in phospholipid bilayers utilizing ^{2}H and ^{15}N solid-state NMR spectroscopy, Biochemistry 43 (2004) 13899–13909.
[45] C.B. Karim, T.L. Kirby, Z.W. Zhang, Y. Nesmelov, D.D. Thomas, Phospholamban structural dynamics in lipid bilayers probed by a spin label rigidly coupled to the peptide backbone, Proc. Natl. Acad. Sci. U. S. A. 101 (2004) 14437–14442.
[46] P.L. Gor'kov, E.Y. Chekmenev, C. Li, M. Cotten, J.J. Buffy, N.J. Traaseth, G. Veglia, W. W. Brey, Using low-E resonators to reduce RF heat in biological samples for static solid-state NMR up to 900 MHz, J. Magn. Reson. 185 (2007) 77–93.
[47] A.D. Wegener, L.R. Jones, Phosphorylation-induced mobility shift in phospholamban in sodium dodecyl sulfate-polyacrylamide gels. Evidence for a protein structure consisting of multiple identical phosphorylatable subunits, J. Biol. Chem. 259 (1984) 1834–1841.
[48] R.L. Cornea, L.R. Jones, J.M. Autry, D.D. Thomas, Mutation and phosphorylation change the oligomeric structure of phospholamban in lipid bilayers, Biochemistry 36 (1997) 2960–2967.
[49] K. Oxenoid, A.J. Rice, J.J. Chou, Comparing the structure and dynamics of phospholamban pentamer in its unphosphorylated and pseudo-phosphorylated states, Protein Sci. 16 (2007) 1977–1983.
[50] S.J. Opella, F.M. Marassi, Structure determination of membrane proteins by NMR spectroscopy, Chem. Rev. 104 (2004) 3587–3606.
[51] F.A. Kovacs, J.K. Denny, Z. Song, J.R. Quine, T.A. Cross, Helix tilt of the M2 transmembrane peptide from influenza A virus: an intrinsic property, J. Mol. Biol. 295 (2000) 117–125.
[52] M. Hong, T. Doherty, Orientation determination of membrane-disruptive proteins using powder samples and rotational diffusion: A simple solid-state NMR approach, Chem. Phys. Lett. 432 (2006) 296–300.
[53] S.H. Park, S.J. Opella, Tilt angle of a trans-membrane helix is determined by hydrophobic mismatch, J. Mol. Biol. 350 (2005) 310–318.
[54] D.H. Jones, K.R. Barber, E.W. VanDerLoo, C.W.M. Grant, Epidermal growth factor receptor transmembrane domain: ^{2}H NMR implications for orientation and motion in a bilayer environment, Biochemistry 37 (1998) 16780–16787.
[55] J. Wang, J. Denny, C. Tian, S. Kim, Y. Mo, F. Kovacs, Z. Song, K. Nishimura, Z. Gan, R. Fu, J.R. Quine, T.A. Cross, Imaging membrane protein helical wheels, J. Magn. Reson. 144 (2000) 162–167.
[56] F.M. Marassi, S.J. Opella, A solid-state NMR index of helical membrane protein structure and topology, J. Magn. Reson. 144 (2000) 150–155.
[57] M.F. Mesleh, G. Veglia, T.M. DeSilva, F.M. Marassi, S.J. Opella, Dipolar waves as NMR maps of protein structure, J. Am. Chem. Soc. 124 (2002) 4206–4207.
[58] F.M. Marassi, S.J. Opella, Simultaneous assignment and structure determination of a membrane protein from NMR orientational restraints, Protein Sci. 12 (2003) 403–411.
[59] A.A. De Angelis, S.C. Howell, A.A. Nevzorov, S.J. Opella, Structure determination of a membrane protein with two trans-membrane helices in aligned phospholipid bicelles by solid-state NMR spectroscopy, J. Am. Chem. Soc. 128 (2006) 12256–12267.
[60] P. Henklein, R. Kinder, U. Schubert, B. Bechinger, Membrane interactions and alignment of structures within the HIV-1 Vpu cytoplasmic domain: effect of phosphorylation of serines 52 and 56, FEBS Lett. 482 (2000) 220–224.
[61] C. Aisenbrey, L. Prongidi-Fix, A. Chenal, D. Gillet, B. Bechinger, Side chain resonances in static oriented proton-decoupled ^{15}N solid-state NMR spectra of membrane proteins, J. Am. Chem. Soc. 131 (2009) 6340–6341.
[62] C. Aisenbrey, B. Bechinger, Tilt and rotational pitch angle of membrane-inserted polypeptides from combined N-15 and H-2 solid-state NMR spectroscopy, Biochemistry 43 (2004) 10502–10512.